

Chapter 4

BETATRON TUNE SHIFTS

4.1 Static Transverse Forces

The vertical motion of a beam particle inside a beam obeys the equation of motion

$$\frac{dp_y}{dt} = F_{\text{ext}}(y) + F_{\text{beam}}(y, \bar{y}) , \quad (4.1)$$

where $p_y = \gamma mdy/dt$ is the vertical momentum of the particle and m its rest mass*. Since we want to study the motion of small vertical displacement y , the Lorentz factor γ can therefore be taken out of the derivative. Here, $F_{\text{ext}}(y)$ is the force due to the magnets outside the vacuum chamber and gives rise to betatron oscillations, while $F_{\text{beam}}(y, \bar{y})$ is the force coming from the electromagnetic fields of the beam on the particle at y and the beam vertical center at \bar{y} . For example, with quadrupole focusing,

$$F_{\text{ext}}(y) = \frac{B'_y}{B\rho} y , \quad (4.2)$$

where $B'_y = dB_y/dx$ is the gradient of the quadrupole magnetic flux density and $B\rho$ the rigidity of the beam. For the sake of simplicity, this focusing can be assumed to be uniform along the accelerator ring; we can therefore make the replacement

$$\langle F_{\text{ext}}(y) \rangle \longrightarrow -(\nu_0^V \omega_0)^2 y , \quad (4.3)$$

*Here, we concentrate on the transverse motion of the beam particles and ignore their momentum offsets and synchrotron motion. Thus, the revolution period of every particle at every turn is the same. This allows us to use the real time t as the independent variable.

where ν_0^V is the number of vertical oscillations the particle makes in a turn or what we usually call the *bare* vertical betatron tune, while $\omega_0/(2\pi)$ is the revolution frequency. Notice that the average of the external force is proportional to the impulse in one accelerator turn. Now the transverse equation of motion becomes

$$\frac{d^2y}{ds^2} + \frac{(\nu_0^V)^2}{R^2} y = \frac{\langle F_{\text{beam}}(y, \bar{y}) \rangle}{\gamma mv^2}, \quad (4.4)$$

where R is the average radius of the ring. In above, the rigid-bunch and impulse approximations have been applied to the F_{beam} , and we have replaced d/dt by vd/ds with $v = \beta c$ being the velocity of the beam, c the velocity of light, and s the distance measured along the longitudinal path in the ring. In this chapter, we are going to study the steady-state effects of the transverse wake potential on the beam. Therefore, there is no explicit time dependency in $\langle F_{\text{beam}} \rangle$. As will be shown below, the steady-state effects of the wake potential contribute to betatron tune shifts, while the time-dependent effects may excite instabilities.

Since we are interested only in small amount of motion in the vertical direction, the beam force can be Taylor expanded to obtain

$$\frac{d^2y}{ds^2} + \frac{(\nu_0^V)^2}{R^2} y = \frac{1}{\gamma mv^2} \left(\frac{\partial \langle F_{\text{beam}} \rangle}{\partial y} \Big|_{\bar{y}=0} y + \frac{\partial \langle F_{\text{beam}} \rangle}{\partial \bar{y}} \Big|_{y=0} \bar{y} \right), \quad (4.5)$$

The first term on the right side is proportional to the vertical displacement of the witness particle; it therefore constitutes a shift of the vertical betatron tune ν_0^V to become ν_{incoh}^V . When the shift is small[†], we write $(\nu_{\text{incoh}}^V)^2 = (\nu_0^V)^2 + 2\nu_0^V \Delta\nu_{\text{incoh}}^V$ with

$$\Delta\nu_{\text{incoh}}^V = -\frac{R^2}{2\nu_0^V \gamma mv^2} \frac{\partial \langle F_{\text{beam}} \rangle}{\partial y} \Big|_{\bar{y}=0}. \quad (4.6)$$

Since this shift affects an individual beam particle, $\Delta\nu_{\text{incoh}}^V$ is called the vertical *incoherent tune shift*. Thus, the incoherent tune shift can be computed by setting $\bar{y} = 0$ or without any displacement of the center of the whole beam.

Let us come back to Eq. (4.5), the transverse equation of motion. We can write one such equation for each beam particle. Perform an average by adding up these equations and dividing by the total number of beam particles. The result is

$$\frac{d^2\bar{y}}{ds^2} + \frac{(\nu_0^V)^2}{R^2} \bar{y} = \frac{1}{\gamma mv^2} \left(\frac{\partial \langle F_{\text{beam}} \rangle}{\partial y} \Big|_{\bar{y}=0} \bar{y} + \frac{\partial \langle F_{\text{beam}} \rangle}{\partial \bar{y}} \Big|_{y=0} \bar{y} \right). \quad (4.7)$$

[†]When the tune shift is large $\Delta\nu_{\text{incoh}}^V$ on the left side of Eq. (4.6) should be replaced by $\Delta(\nu^V)^2_{\text{incoh}}/(2\nu_0^V)$. The same applies to Eqs. (4.8), (4.13), (4.16), (4.19), etc.

This equation describes the vertical motion of the center of the beam, or the *coherent motion* of the beam, which is just a simple harmonic motion. The vertical betatron tune of the center of the beam, or the *coherent* vertical betatron tune of the beam, is now $\nu_{\text{coh}}^V = \nu_0^V + \Delta\nu_{\text{coh}}^V$. When the perturbation is small, the coherent tune shift becomes

$$\Delta\nu_{\text{coh}}^V = -\frac{R^2}{2\nu_0^V \gamma m v^2} \left(\frac{\partial \langle F_{\text{beam}} \rangle}{\partial y} \Big|_{\bar{y}=0} + \frac{\partial \langle F_{\text{beam}} \rangle}{\partial \bar{y}} \Big|_{y=0} \right). \quad (4.8)$$

Because we keep only the linear terms of the Taylor expansion in Eq. (4.5), we have included only the dipole parts of the wake force. As a result, these tune shifts should be called dipole coherent tune shift and dipole incoherent tune shift.

Let us assume here that the vacuum chamber is completely smooth and infinitely conducting. Then the force on a beam particle from the beam comes from only two sources: (1) electromagnetic interaction of the beam particle with all other beam particles in the beam, which we call *self-force*, (2) reflection of electromagnetic fields from the walls of the vacuum chamber, which we call *image forces*.

4.1.1 Electric Image Forces

The image forces certainly depends on the geometry of the vacuum chamber. Let us consider the simple case when the vacuum chamber consists of two infinite horizontal plates at location $y = \pm h$ as illustrated in Fig. 4.1. The beam of say positive charges is displaced by \bar{y}_1 vertically and the witness particle is at y_1 . We wish to consider the electric force on the witness particle coming from reflection by the top and bottom walls of the vacuum chamber. In order that the horizontal electric field at the top wall vanishes, there must be an image of the beam with negative charges at position $y = 2h - \bar{y}_1$ or at a distance $2h - \bar{y}_1 - y_1$ from the witness particle. In order that the horizontal electric field at the bottom wall vanishes, this image will have another image of positive charges from the bottom wall at $y = -(4h - \bar{y}_1)$ or $4h - \bar{y}_1 + y_1$ from the witness particle. This secondary image will have a third image of negative charges from the top wall, a 4th image of positive charges from the bottom wall, etc.

Similarly, the beam has an image of negative charges first from the bottom wall at $y = -(2h + \bar{y}_1)$ or $2h + \bar{y}_1 + y_1$ from the witness particle. This image will form another image of positive charges through the top wall with positive charges at $y = 4h + \bar{y}_1$ or $4h + \bar{y}_1 - y_1$ from the witness particle, etc. Summing up, the vertical electric field acting

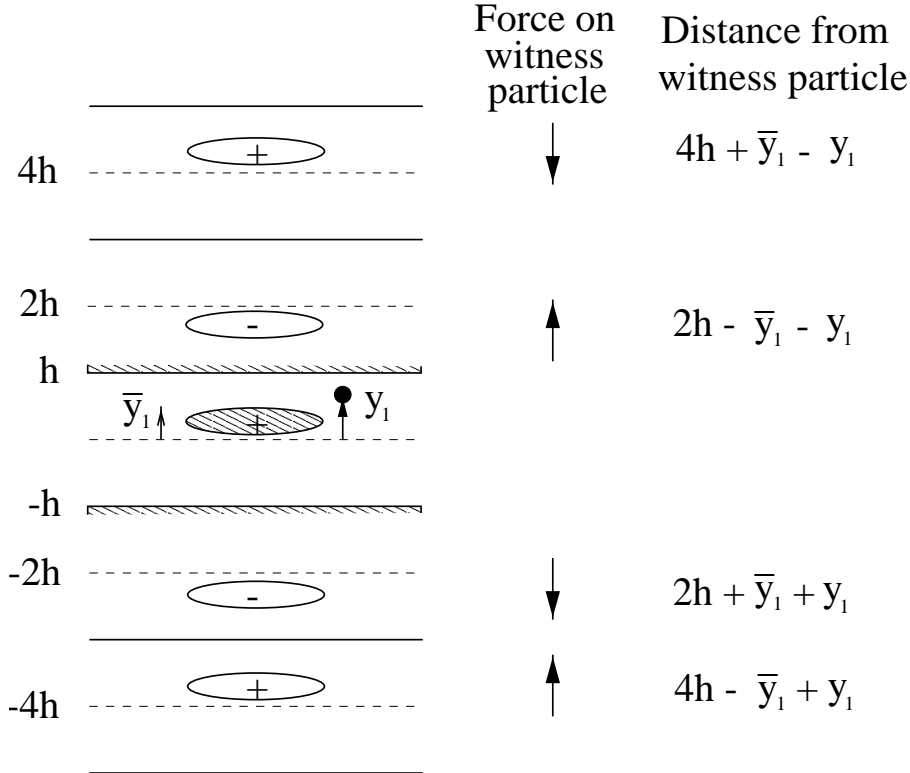


Figure 4.1: Illustration showing the electric forces from the images of a beam, off centered vertically by \bar{y}_1 , acting on a witness particle at location y_1 inside the beam between two infinite horizontal conducting parallel plates separated vertically by distance $2h$.

on the witness particle is, according to Gauss's law in the cylindrical coordinates,

$$E_y = \frac{e\lambda}{2\pi\epsilon_0} \left[+ \frac{1}{2h - \bar{y}_1 - y_1} - \frac{1}{2h + \bar{y}_1 + y_1} + \frac{1}{6h - \bar{y}_1 - y_1} - \frac{1}{6h + \bar{y}_1 + y_1} + \dots - \frac{1}{4h + \bar{y}_1 - y_1} + \frac{1}{4h - \bar{y}_1 + y_1} - \frac{1}{8h - \bar{y}_1 - y_1} + \frac{1}{8h + \bar{y}_1 + y_1} + \dots \right], \quad (4.9)$$

where λ is the linear particle density per unit length along the ring. Every two adjacent terms are grouped together giving

$$E_y = \frac{e\lambda}{2\pi\epsilon_0} \left[+ \frac{2(\bar{y}_1 + y_1)}{(2h)^2 - (\bar{y}_1 + y_1)^2} + \frac{2(\bar{y}_1 + y_1)}{(6h)^2 - (\bar{y}_1 + y_1)^2} + \dots + \frac{2(\bar{y}_1 - y_1)}{(4h)^2 - (\bar{y}_1 - y_1)^2} + \frac{2(\bar{y}_1 - y_1)}{(8h)^2 - (\bar{y}_1 - y_1)^2} + \dots \right]. \quad (4.10)$$

Since we consider only small vertical motion, only terms linear in $\bar{y}_1 + y_1$ and $\bar{y}_1 - y_1$ are kept leading to

$$\begin{aligned} E_y &= \frac{e\lambda}{\pi\epsilon_0 h^2} \left[(\bar{y}_1 + y_1) \left(\frac{1}{2^2} + \frac{1}{6^2} + \frac{1}{10^2} + \dots \right) + (\bar{y}_1 - y_1) \left(\frac{1}{4^2} + \frac{1}{8^2} + \frac{1}{12^2} + \dots \right) \right] \\ &= \frac{e\lambda}{\pi\epsilon_0 h^2} \left[(\bar{y}_1 + y_1) \frac{\pi^2}{32} + (\bar{y}_1 - y_1) \frac{\pi^2}{96} \right]. \end{aligned} \quad (4.11)$$

In the literature, there is a standard way to write these image contributions following the work of Laslett [1, 2, 3]:

$$E_y = \frac{e\lambda}{\pi\epsilon_0} \frac{\epsilon_1^V}{h^2} y_1 \quad \text{and} \quad \frac{e\lambda}{\pi\epsilon_0} \frac{\xi_1^V}{h^2} \bar{y}_1, \quad (4.12)$$

where ϵ_1^V and ξ_1^V are called, respectively, the incoherent and coherent *electric image coefficients*. For the situation of two parallel plates, we have $\epsilon_1^V = \pi^2/48$ and $\xi_1^V = \pi^2/16$. Attention should be paid that in deriving the coherent image coefficient, y_1 has been replaced by \bar{y}_1 in Eq. (4.9) or (4.10) or (4.11). According to Eqs. (4.6) and (4.8), the coherent and incoherent vertical tune shifts due to electric images are:

$$\Delta\nu_{\text{incoh}}^V = -\frac{Nr_0R}{\pi\gamma\beta^2\nu_0^V} \frac{\epsilon_1^V}{h^2} \quad \text{and} \quad \Delta\nu_{\text{coh}}^V = -\frac{Nr_0R}{\pi\gamma\beta^2\nu_0^V} \frac{\xi_1^V}{h^2}, \quad (4.13)$$

where we have replaced the linear particle density by $\lambda = N/(2\pi R)$ with N being the total number of particles in the beam, and introduced the classical radius of the particle $r_0 = e^2/(4\pi\epsilon_0 mc^2)$.

Notice that there is a negative sign in front of each of the tune shift expressions in Eq. (4.13). This implies that a positive image coefficient will contribute a downward shifting to the betatron tune.

4.1.2 Magnetic Image Forces

Unlike the electric field that cannot penetrate the metallic vacuum chamber at any frequency, the effect of the magnetic field is more complex. The magnet field has an ac component and a dc component. The ac component has its component parallel to the wall of the vacuum chamber converted into eddy current. In other words, the ac magnetic field *cannot* penetrate the wall of the vacuum chamber. There the boundary condition is $B_\perp = 0$, or the magnetic flux density B is parallel to the wall of the vacuum

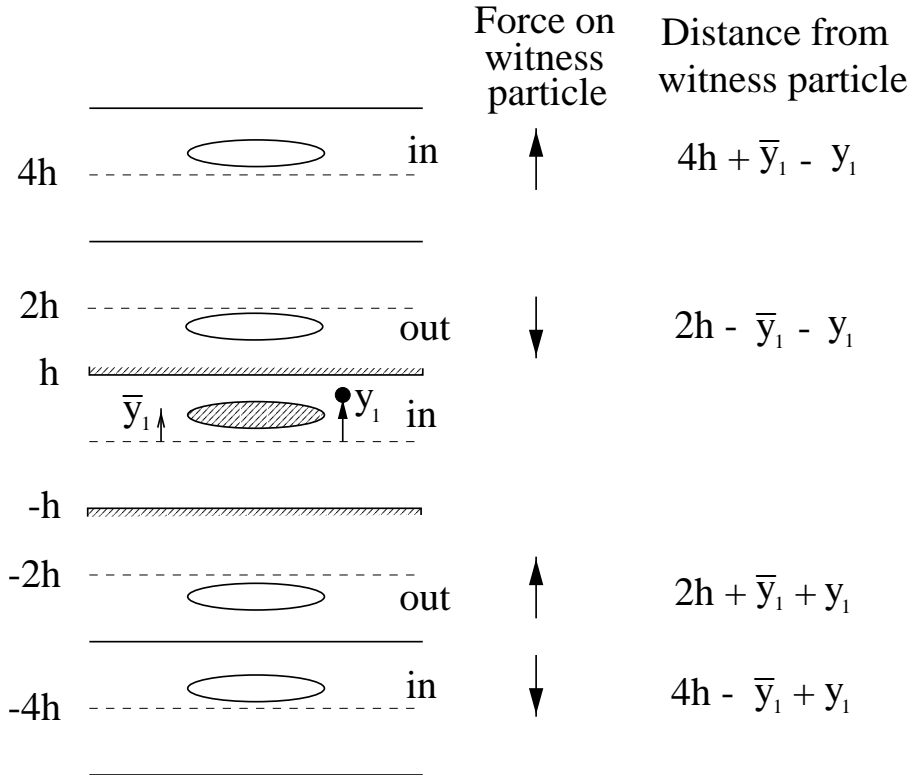


Figure 4.2: Illustration showing the magnetic forces from the images of a beam, off centered vertically by \bar{y}_1 , acting on a witness current at location y_1 inside the beam between two infinite horizontal conducting parallel plates separated vertically by distance $2h$. The normal components of the non-penetrating magnetic fields vanish at the plates. The beam or image currents flowing into or out of the paper are labeled “in” or “out”.

chamber. To accomplish this, the first image from a boundary wall gives an image current that flows in the opposite direction to that the beam. The total force from these magnetic images acting on the witness charge current at position y_1 is illustrated in Fig. 4.2 and is expressed as

$$\frac{F_y^{\text{mag}}}{e} = -\frac{e\mu_0\lambda v^2}{2\pi} \left[+\frac{1}{2h-\bar{y}_1-y_1} - \frac{1}{2h+\bar{y}_1+y_1} + \frac{1}{6h-\bar{y}_1-y_1} - \frac{1}{6h+\bar{y}_1+y_1} + \dots - \frac{1}{4h+\bar{y}_1-y_1} + \frac{1}{4h-\bar{y}_1+y_1} - \frac{1}{8h-\bar{y}_1-y_1} + \frac{1}{8h+\bar{y}_1+y_1} + \dots \right]. \quad (4.14)$$

There is the factor v^2 outside the square brackets on the right side. One v comes from the source beam current and the other v comes from the Lorentz force. It is interesting to see that the factor outside the square brackets is equal to $-e\lambda\beta^2/(2\pi\epsilon_0)$. Thus, the force due to the ac magnetic images are equal to the force due to the electric images multiplied by the factor $-\beta^2$. This leads to

$$\frac{F_y^{\text{mag}}}{e} = -\frac{e\lambda\beta^2}{2\pi\epsilon_0 h^2} \left[(\bar{y}_1 + y_1) \frac{\pi^2}{32} + (\bar{y}_1 - y_1) \frac{\pi^2}{96} \right]. \quad (4.15)$$

Following Eq. (4.13), tune shifts due to ac magnetic images can be expressed as terms of the former electric image coefficients ϵ_1^V and ξ_1^V :

$$\Delta\nu_{\text{incoh}}^V = \frac{Nr_0R}{\pi\gamma\nu_0^V} \frac{\epsilon_1^V}{h^2} \quad \text{and} \quad \Delta\nu_{\text{coh}}^V = \frac{Nr_0R}{\pi\gamma\nu_0^V} \frac{\xi_1^V}{h^2}. \quad (4.16)$$

There is always a dc part of the magnetic field that can penetrate the wall of the beam pipe and lands on the pole faces of the magnet as if the vacuum chamber were not there. The boundary condition on the magnet pole faces is now B_\perp continuous and $B_\parallel = 0$. In order to accommodate this, all the image currents must flow in exactly the same direction of the source beam, as illustrated in Fig. 4.3. The force on the witness particle is now

$$\begin{aligned} \frac{F_y^{\text{mag}}}{e} = & \frac{e\mu_0\lambda v^2}{2\pi} \left[+ \frac{1}{2g - \bar{y}_1 - y_1} - \frac{1}{2g + \bar{y}_1 + y_1} + \frac{1}{6g - \bar{y}_1 - y_1} - \frac{1}{6g + \bar{y}_1 + y_1} + \dots \right. \\ & \left. + \frac{1}{4g + \bar{y}_1 - y_1} - \frac{1}{4g - \bar{y}_1 + y_1} + \frac{1}{8g - \bar{y}_1 - y_1} - \frac{1}{8g + \bar{y}_1 + y_1} + \dots \right], \end{aligned} \quad (4.17)$$

where the magnetic pole faces are at $y = \pm g$ or the magnets have a vertical gap $2g$ between the poles faces. It is important to note the slight difference between Eqs. (4.14) and (4.17). Here we obtain

$$\frac{F_y^{\text{mag}}}{e} = +\frac{e\lambda\beta^2}{2\pi\epsilon_0 g^2} \left[(\bar{y}_1 + y_1) \frac{\pi^2}{32} - (\bar{y}_1 - y_1) \frac{\pi^2}{96} \right], \quad (4.18)$$

as compared to Eq. (4.15). Following Laslett, we write the tune shifts due to dc magnetic images as

$$\Delta\nu_{\text{incoh}}^V = -\frac{Nr_0R}{\pi\gamma\nu_0^V} \frac{\epsilon_2^V}{g^2} \quad \text{and} \quad \Delta\nu_{\text{coh}}^V = -\frac{Nr_0R}{\pi\gamma\nu_0^V} \frac{\xi_2^V}{g^2}, \quad (4.19)$$

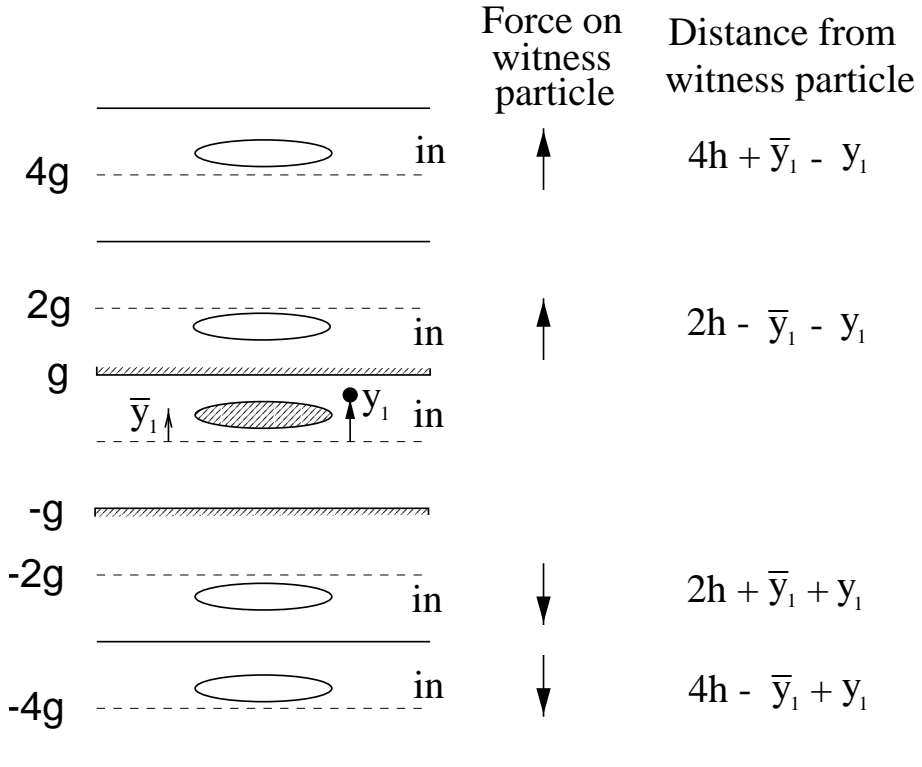


Figure 4.3: Illustration showing the magnetic forces from the images of a beam, off centered vertically by \bar{y}_1 , acting on a witness current at location y_1 inside the beam between two infinite horizontal parallel pole faces separated vertically by distance $2g$. The parallel components of the penetrating magnetic fields vanish at the pole faces. Here, the beam and all image currents flow into the paper.

where ϵ_2^V and ξ_2^V are called, respectively, the vertical incoherent and coherent dc *magnetic image coefficients*. For the special case of two parallel plates, they assume the values $\epsilon_2^V = \pi^2/24$ and $\xi_2^V = \pi^2/16$.

There is also a set of horizontal image coefficients: ϵ_1^H , ϵ_2^H , ξ_1^H , and ξ_2^H . Because the image forces acting on the witness particle come directly from the individual images, the electric field and magnetic flux density from the images at the location of the witness particle satisfy source-free Gauss's law, or $\vec{\nabla} \cdot \vec{E} = 0$ and $\vec{\nabla} \cdot \vec{B} = 0$. We therefore always have

$$\epsilon_1^H = -\epsilon_1^V \quad \text{and} \quad \epsilon_2^H = -\epsilon_2^V. \quad (4.20)$$

On the other hand, there is no definite relationship between the horizontal and vertical

coherent electric image coefficients. In the special case of two parallel plates, it is obvious that $\xi_1^H = 0$ and $\xi_2^H = 0$, which is the result of translational invariance. For a beam pipe with circular cross section or square cross section, $\epsilon_1^H = 0$ and $\epsilon_2^H = 0$ because of symmetry between the horizontal and vertical.

It is important to point out that electric and magnetic image coefficients are always defined with reference to the square of the *half vertical* vacuum chamber h or the square of the *half vertical* magnetic pole gap g , independent of whether we are talking about the vertical or horizontal tune shifts. For the example of a rectangular beam pipe of half height h and half width w , only h^2 will enter into the denominators but never w^2 , such as in Eqs. (4.13), (4.16), or (4.19). In the same way, for an elliptical beam pipe of vertical radius b and horizontal radius a , the image coefficients will be defined with reference to $h = b$ but not a . It is because of such a dedicated reference that the relations in Eq. (4.20) hold.

4.1.3 Space charge Self-Forces

The interaction of a beam particle with other beam particles in the beam depends on the transverse distribution of the beam. Let us first consider a uniformly distributed coasting beam of circular cross section and radius a . The witness particle at $y = y_1 \leq a$ sees, in the y -direction, an electric force[†]

$$F_y^{\text{elect}} = \frac{e^2 \lambda}{2\pi\epsilon_0 a^2} (y_1 - \bar{y}_1) , \quad (4.21)$$

and a magnetic force

$$F_y^{\text{mag}} = -\frac{e^2 \mu_0 \lambda v^2}{2\pi a^2} (y_1 - \bar{y}_1) = -\frac{e^2 \lambda \beta^2}{2\pi\epsilon_0 a^2} (y_1 - \bar{y}_1) , \quad (4.22)$$

or a total force of

$$F_y = \frac{e^2 \lambda}{2\pi\epsilon_0 \gamma^2 a^2} (y_1 - \bar{y}_1) . \quad (4.23)$$

where \bar{y}_1 is vertical position of the center of the beam. This self-force is a space charge force. According to Eq. (4.6), this self-force leads to a space charge tune shift of

$$\Delta\nu_{\text{spch coh}}^{V,H} = -\frac{Nr_0 R}{2\pi\gamma^3 \beta^2 a^2 \nu_0^{V,H}} . \quad (4.24)$$

[†]The vertical electric and magnetic forces in Eqs. (4.21) and (4.22) are true for any particle at a vertical distance $y = y_1 \leq a$ above the center of the beam and are independent of the particle horizontal position.

It is clear from Eq. (4.23) that the coherent space charge tune shifts in both transverse directions are zero. This is understandable, because the center of the beam does not see its own space charge force. We can also define the self-field or space charge coefficients in the vertical and horizontal directions, $\epsilon_{\text{spch}}^{V,H} = \frac{1}{2}$, such that

$$\Delta\nu_{\text{spch incoh}}^{V,H} = -\frac{Nr_0R}{\pi\gamma^3\beta^2\nu_0^{V,H}}\frac{\epsilon_{\text{spch}}^{V,H}}{a^2}. \quad (4.25)$$

The space charge coefficients take care of the transverse shape of the beam and how the beam particles are distributed.

Now consider a beam with uniform transverse distribution but elliptical cross section with vertical and horizontal radii a_V and a_H . In defining the space charge coefficients, we follow the same convention of the Laslett image coefficients that the a^2 in the denominator of Eq. (4.25) is always a_V^2 , independent of whether we are referring to the vertical or horizontal space charge tune shift. The vertical and horizontal space charge coefficients are then (Exercise 4.3)

$$\epsilon_{\text{spch}}^V = \frac{a_V}{a_V + a_H} \quad \text{and} \quad \epsilon_{\text{spch}}^H = \frac{a_V^2}{a_H(a_V + a_H)}. \quad (4.26)$$

These coefficients become $\frac{1}{2}$ when $a_V = a_H$ as expected.

We can also express the incoherent space charge tune shift in term of the normalized emittance of the beam

$$\epsilon_N^{V,H} = \gamma\beta \frac{a_{V,H}^2}{\langle\beta_{V,H}\rangle}, \quad (4.27)$$

where $\langle\beta_{V,H}\rangle$ is the average vertical/horizontal betatron function of the ring, which is roughly equal to $R/\nu_0^{V,H}$. Then, we have

$$\Delta\nu_{\text{spch incoh}}^{V,H} = -\frac{Nr_0}{\pi\gamma^2\beta\sqrt{\epsilon_N^{V,H}}\left(\sqrt{\epsilon_N^{V,H}} + \sqrt{\epsilon_N^{H,V}\langle\beta_{H,V}\rangle/\langle\beta_{V,H}\rangle}\right)B}. \quad (4.28)$$

In the above, we have also introduced the single-bucket bunching factor B to take care of the fact the the beam may be longitudinally bunched. The single-bucket bunching factor is defined as

$$B = \frac{I_{\text{av}}}{I_{\text{pk}}}, \quad (4.29)$$

where I_{av} and I_{pk} are, respectively, the current of a bunch averaged over a *single* rf bucket and its peak current, or the average current to the peak current assuming that all the buckets are filled.

We can also consider a beam with cylindrical cross section but with transverse bi-Gaussian distribution,

$$f(x, y) = \frac{\lambda}{2\pi\sigma^2} e^{-(x^2+y^2)/(2\sigma^2)} , \quad (4.30)$$

where σ is the rms transverse spread of the beam and $\lambda = N/(2\pi R)$ is the linear density. A particle at $y = y_1$ vertically above the center of the beam sees an electric force in the y direction,

$$F_y^{\text{elect}} = \frac{e^2}{2\pi\epsilon_0 y_1} \frac{\lambda}{\sigma^2} \int_0^{y_1} e^{-r^2/(2\sigma^2)} r dr = \frac{e^2 \lambda}{2\pi\epsilon_0 y_1} \left[1 - e^{-y_1^2/(2\sigma^2)} \right] . \quad (4.31)$$

For small offset, $y_1 \ll \sigma$, we have

$$F_y^{\text{elect}} = \frac{e^2 \lambda}{4\pi\epsilon_0 \sigma^2} y_1 . \quad (4.32)$$

The magnetic force is the same but multiplied by $-\beta^2$. The incoherent space charge tune shift is therefore

$$\Delta\nu_{\text{spch incoh}}^{V,H} = -\frac{Nr_0R}{4\pi\gamma^3\beta^2\sigma^2\nu_0^{V,H}} . \quad (4.33)$$

Here, we can define the 95% normalized transverse emittance $\epsilon_{N95}^{V,H}$ of the beam which encloses 95% of the beam particles. This corresponds to a radius r_{95} given by

$$\frac{1}{2\pi\sigma^2} \int_0^{r_{95}} e^{-r^2/(2\sigma^2)} 2\pi r dr = 95\% , \quad (4.34)$$

which gives $r_{95} \approx \sqrt{6}\sigma$. Thus

$$\epsilon_{N95}^{V,H} = \gamma\beta \frac{r_{95}^2}{\langle\beta_{V,H}\rangle} \approx \gamma\beta \frac{6\sigma^2}{\langle\beta_{V,H}\rangle} . \quad (4.35)$$

The space charge tune shift becomes

$$\Delta\nu_{\text{spch incoh}}^{V,H} = -\frac{3Nr_0}{2\pi\gamma^2\beta\epsilon_{N95}^{V,H}B} . \quad (4.36)$$

In general, if the beam has an elliptical cross section with vertical/horizontal rms beam size $\sigma_{V,H}$, the space charge coefficients for a particular beam particle can be represented by

$$\epsilon_{\text{spch}}^V = \frac{f\sigma_V}{\sigma_V + \sigma_H} \quad \text{and} \quad \epsilon_{\text{spch}}^H = \frac{f\sigma_V^2}{\sigma_H(\sigma_V + \sigma_H)} , \quad (4.37)$$

where the form factor f comes about because each particle in a transverse slice of the beam receives different tune shifts. For the bi-Gaussian distribution, if we consider only the particles at the center of the beam where the tune shifts are largest, $f = 3$. Thus the tune shift is three times as large as the tune shift for a uniform distribution in Eq. (4.28). This is because particles are mostly concentrated near the bunch center in a bi-Gaussian distribution and the linear particle density at the bunch center is therefore much larger. However, the tune shift for those particles with transverse offsets will be much smaller. If we make a rough model by assuming those particles within one sigma of the beam core to have the maximum tune shift while those outside do not experience any space charge force, we obtain some sort of average for the particles in the cross sectional slice, $f = 3(1 - e^{-1/2}) = 1.180$, which is only slightly larger than that for a uniformly distributed beam.

It is important to point out that what we really care for is the spread in space charge tune shift among the particles inside the beam, but not so much the maximum space charge tune shift, because the latter can be corrected by changing the bare tune of the machine. For a distribution of finite extent, the space charge tune spread is always less than the maximum space charge tune spread, which occurs at the center of the beam for most distributions. For a transverse bi-Gaussian distribution that extend to infinity, the space charge tune shift of a particle infinitely far away from the beam axis is zero, and therefore the space charge tune spread is equal to the maximum space charge tune shift. However, these particles are excluded from a realistic distribution which has a finite extent and this makes the space charge tune spread less than the maximum tune shift. When the bi-Gaussian distribution is truncated more and more (by including only those particles closer and closer to the beam center), the space charge tune spread becomes smaller and smaller while the maximum space charge tune shift remains unchanged. For a round beam, with bi-Gaussian distribution, $\sigma_r = \sigma_H = \sigma_V$ and maximum excursion r , the form factor $f(r/\sigma_r)$ in Eq. (4.37) for betatron amplitude r is found to be

$$\frac{f(r/\sigma_r)}{3} = \frac{8\sigma_r^2}{\pi r^2} \int_0^{\pi/2} \left[1 - \exp \left(-\frac{r^2}{2\sigma_r^2} \sin^2 \theta \right) \right] d\theta = \sum_{n=1}^{\infty} \frac{(2n)!}{2(n!)^3} \left(-\frac{r^2}{8\sigma_r^2} \right)^{n-1}, \quad (4.38)$$

which is depicted in Fig. 4.4. Consider a beam with a bi-Gaussian distribution truncated at $2.5\sigma_r$, we see that the particles at the edge of the beam have a space charge tune shift $\sim 40\%$ of the maximum space charge tune shift. Thus the space charge tune spread is equal to $\sim 60\%$ the maximum space charge tune shift. On the other hand, for the uniform transverse distribution, the space charge tune shift is amplitude independent and the spread is zero exactly.

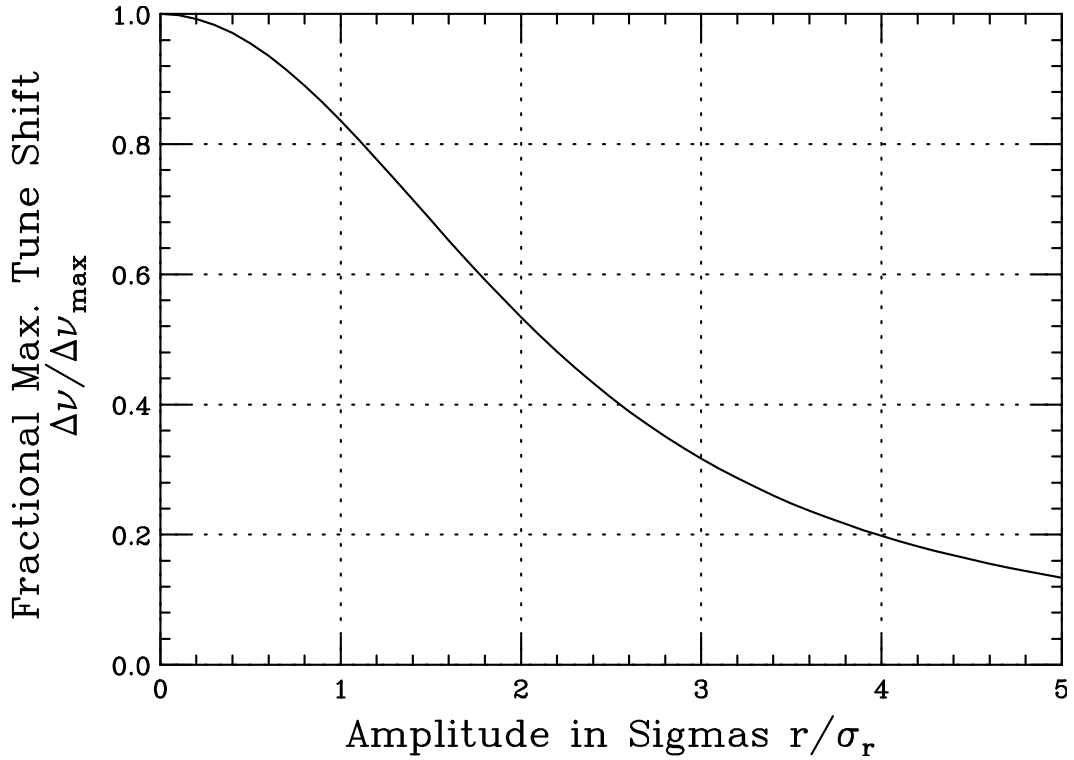


Figure 4.4: Plot of space charge tune shift of a particle with betatron amplitude r as a fraction of the maximum space charge tune shift of a bi-Gaussian distributed round beam with rms beam size σ_r .

We now understand that the space charge self-force of a bunch acting on the individual beam particles constitutes vertical and horizontal tune spreads. Usually, people say that large incoherent space charge tune spreads will encompass a lot of parametric resonances in the ν^V - ν^H tune space and lead to instability. For this reason, the beam intensities in low-energy synchrotrons are limited by the horizontal and vertical space charge tune spreads. The common rule of thumb is that incoherent self-field tune spreads should not exceed ~ 0.40 . At the same time, the widths of important stopbands should also be minimized by corrections made to the ring lattice. However, these self-field tune spreads at injection have never been well-measured beam parameters. It is difficult to measure because low-energy rings are usually ramped very rapidly. Thus, the self-field tune spreads diminish very quickly as the energy of the beam increases. Most low-energy rings that have large space charge tune spreads are ramped by resonators. To measure the self-field tune spreads, we must disconnect the magnet winding currents from the resonator so as to provide a longer interval for which the beam energy does not change.

This is not always possible, because the beam will generally become unstable if it is allowed to stay at such low energy for a long time. If the condition is available, however, the tune spreads can be measured by a technique called rf knockout. A narrow band rf signal is used to excite the beam. Those particles with the correct tune resonate with the driving signal and are lost. Since only a small fraction of the beam resonates, this resonating frequency of rf signal corresponds to the incoherent tune of the beam. Another way is to perform a Schottky scan which shows the tunes of individual particles. The coherent tune shifts can be measured by the same rf knockout method. If the exciting rf signal hits a coherent tune, the whole beam will be lost.

As we shall see in Chapter 5 that it is the *coherent* rather than the *incoherent* tune shifts that determine the instability of a beam. In fact, this is quite reasonable. When the bunch is oscillating at an integer coherent tune, we have the usual integer resonance. This leads to an instability because all particles are performing betatron oscillations with a tune component that is at an integer. The whole beam will become unstable. Although the dipole coherent space charge tune shift vanishes because the beam moves rigidly, there are other coherent motion of the beam, for example when the beam size oscillates without the beam center being moved. Some of these modes will be derived after introducing the envelope equation.

One may argue that if the incoherent tune spread covers an integer or half-integer resonance, *a small amount* of particles are hitting the resonance, and this small amount of the beam will be unstable. It will be shown in Chapter 5 that even this statement is incorrect, because the space charge self-force vanishes when the incoherent motion of the beam particles hit a resonance. Then why should we study the incoherent space charge tune shift if the resonances have nothing to do with incoherent motion? The answer is: the higher-multipole coherent space charge tune shifts depend on the incoherent space charge tune shift. Thus, if the incoherent space charge tune shift can be controlled, say by blowing up the transverse beam size, the higher-multipole coherent space charge tune shifts will become smaller also. In this way, a higher intensity beam will be possible before hitting the parametric resonances.

4.2 Tune Shift for a Beam

In this section, we want to derive the general expressions of incoherent and coherent tune shifts for a beam, unbunched or bunched, in terms of Laslett image coefficients and the self-force coefficients. These expressions are complicated by the fact that the magnetic field may or may not penetrate the vacuum chamber.

4.2.1 Image Formation

Let us recall how images of the beam are formed, in the walls of the vacuum chamber? or in the magnetic pole faces? For the electric field, because the parallel component vanishes on the walls of the vacuum chamber which we assume to be infinitely conducting, images will always be formed in the walls of the vacuum chamber. We therefore say that electric field is always *non-penetrating*. In this discussion, *penetrating* or *non-penetrating* always implies penetrating or non-penetrating the vacuum chamber.

The magnetic field is quite different. All low-frequency magnetic field will penetrate the vacuum chamber and form images in the magnet pole faces. If no magnet pole faces are present, we assume that magnetic field will go to infinity and will no longer affect the test particle. All high-frequency magnetic field will not penetrate the vacuum chamber and form images in the walls of the vacuum chamber.

Before proceeding further, there is an important rule that is worth mentioning. For images in the wall of the vacuum chamber, we use the *electric* image coefficient $\epsilon_1^{V,H}$ or $\xi_1^{V,H}$, depending on whether it is incoherent or coherent. The electric image coefficients are used not only for electric images but also for magnetic images. The only difference is that, for magnetic images, we use $-\beta^2\epsilon_1^{V,H}$ or $-\beta^2\xi_1^{V,H}$. This is because the actual contribution of magnetic field from the images in the walls of the vacuum chamber is exactly the same as the electric field. The factor β^2 comes about because we need a factor of β from the magnetic part of the Lorentz force and another factor of β from the source which is the beam current. The negative sign comes about because the magnetic force on a beam is always in opposite direction to the electric force. As for images formed in the magnet pole faces, they can only be magnetic images, because electric field cannot penetrate the vacuum chamber. Their contributions will be $\beta^2\epsilon_2^{V,H}$ or $\beta^2\xi_2^{V,H}$, respectively, when the tune shifts are incoherent or coherent. Here we have the same factor of β^2 . However, there is *no negative sign*, which is just a convention.

In other words, one may consider the negative sign to have been absorbed into the definition of $\beta^2\epsilon_2^{V,H}$ or $\beta^2\xi_2^{V,H}$. We can also say that electric image coefficients are for images in the walls of the vacuum chamber independent of whether the effect is electric or magnetic, while magnetic image coefficients are for images in the magnet pole faces. All these considerations are summarized in Table 4.1, where we also separate the coherent tune shift in Eq. (4.8) into two parts: the dc part $\partial\langle F_{\text{beam}} \rangle / \partial y|_{\bar{y}=0}$ when the beam is stationary and the ac part $\partial\langle F_{\text{beam}} \rangle / \partial \bar{y}|_{y=0}$ when the beam is oscillating.

Table 4.1: Relation of each component of the beam force to the image coefficients with images formed in the vacuum chamber or magnetic pole faces.

Beam force components	Images in vacuum chamber		Comments
	electric	magnetic	
$\frac{\partial\langle F_{\text{beam}} \rangle}{\partial y} \Big _{\bar{y}=0}$	$\frac{\epsilon_1^{V,H}}{h^2}$	$-\beta^2 \frac{\epsilon_1^{V,H}}{h^2}$	$\beta^2 \frac{\epsilon_2^{V,H}}{g^2}$ incoherent dc coherent
$\frac{\partial\langle F_{\text{beam}} \rangle}{\partial y} \Big _{\bar{y}=0} + \frac{\partial\langle F_{\text{beam}} \rangle}{\partial \bar{y}} \Big _{y=0}$	$\frac{\xi_1^{V,H}}{h^2}$	$-\beta^2 \frac{\xi_1^{V,H}}{h^2}$	$\beta^2 \frac{\xi_2^{V,H}}{g^2}$ coherent
$\frac{\partial\langle F_{\text{beam}} \rangle}{\partial y} \Big _{y=0}$		$-\beta^2 \frac{\xi_1^{V,H} - \epsilon_1^{V,H}}{h^2}$	$\beta^2 \frac{\xi_2^{V,H} - \epsilon_2^{V,H}}{g^2}$ ac coherent

4.2.2 Coasting Beams

Now we are ready to express the tune shifts in terms of image coefficients. First, let us study the simpler case of a coasting beam, where the only ac magnetic field comes from betatron oscillations. The frequency will be low when the betatron tune is close to an integer and the magnetic field may be penetrating. On the other hand, the frequency will be high when the betatron tune is close to a half integer and the magnetic field may be non-penetrating. The incoherent tune shifts are:

$$\Delta\nu_{\text{incoh}}^{V,H} = -\frac{Nr_0R}{\pi\gamma\beta^2\nu_0^{V,H}} \left[\frac{\epsilon_1^{V,H}}{h^2} + \mathcal{F}\beta^2 \frac{\epsilon_2^{V,H}}{g^2} + (1-\beta^2) \frac{\epsilon_{\text{spch}}^{V,H}}{a_V^2} \right]. \quad (4.39)$$

\uparrow \uparrow \uparrow
 electric image magnetic image self-field, $(1-\beta^2)$ gives
 in vacuum chamber in magnet poles balance between E and \vec{H}

Here, the first term comes from the electric images in the vacuum chamber since electric field is always non-penetrating and therefore the incoherent electric image coefficient $\epsilon_1^{V,H}/h^2$. The second term comes the magnetic images in the magnet pole faces and therefore the incoherent magnetic image coefficient $\epsilon_2^{V,H}$ together with the factor β^2 in front and g^2 in the denominator. The factor \mathcal{F} represents the fraction of the ring circumference where the beam is sandwiched between magnetic pole faces. As stated before, the incoherent beam force comes from the images of the beam center which is not displaced or $\bar{y} = 0$. These images are not moving and the beam force is therefore static or dc, and the magnetic field is therefore landing on the magnet pole faces. The last term is just the space charge contribution, where the 1 denotes the electric part and $-\beta^2$ the magnetic part.

For the coherent tune shifts of a coasting beam, if the magnetic field is penetrating, we just have simply,

$$\Delta\nu_{\text{coh}}^{V,H} = -\frac{Nr_0R}{\pi\gamma\beta^2\nu_0^{V,H}} \left[\frac{\xi_1^{V,H}}{h^2} + \mathcal{F}\beta^2 \frac{\xi_2^{V,H}}{g^2} \right], \quad (4.40)$$

↑
↑

electric image
magnetic image

in vacuum chamber
in magnet poles

where all the magnetic field penetrates the vacuum chamber and forms images in the magnet pole faces. Note that there is no space charge term because the center of the beam does not see the self-force among beam particles.

When the magnetic field is non-penetrating, we have instead

$$\Delta\nu_{\text{coh}}^{V,H} = -\frac{Nr_0R}{\pi\gamma\beta^2\nu_0^{V,H}} \left[\frac{\xi_1^{V,H}}{h^2} + \mathcal{F}\beta^2 \frac{\epsilon_2^{V,H}}{g^2} - \beta^2 \frac{\xi_1^{V,H} - \epsilon_1^{V,H}}{h^2} \right]. \quad (4.41)$$

↑
↑
↑

electric image
magnetic image
ac magnetic image

in vacuum chamber
in magnet poles
in vacuum chamber

To understand this expression, recall the magnetic part of beam force on the right side of Eq. (4.5). The ac magnetic field comes from the betatron oscillation of the whole beam and has its source from the second term on the right side only, since we require a moving beam center or $\bar{y} \neq 0$. According to Table 4.1, the contribution is therefore $-\beta^2(\xi_1^{V,H} - \epsilon_1^{V,H})/h^2$. The dc part of the coherent magnet beam force is the first term on the right side of Eq. (4.5). Since this dc field produces images in the magnet pole faces,

we have therefore the second term of Eq. (4.41). The first term comes from the electric component of the coherent beam force. After re-arrangement, the coherent tune shift with penetrating fields reads

$$\Delta\nu_{\text{coh}}^{V,H} = -\frac{Nr_0R}{\pi\gamma\beta^2\nu_0^{V,H}} \left[\frac{(1-\beta^2)\xi_1^{V,H}}{h^2} + \beta^2\frac{\epsilon_1^{V,H}}{h^2} + \mathcal{F}\beta^2\frac{\epsilon_2^{V,H}}{g^2} \right]. \quad (4.42)$$

4.2.3 Bunched Beams

For bunched beam, we would like to compute the maximum tune shifts when the beam current is at its local maximum. We therefore divide by the bunching factor B suitably so that the bunch intensity will be properly enhanced. Notice that ac magnetic field now comes from two sources: transverse betatron oscillation of the bunch and longitudinal or axial bunching of the beam. Although both effects are ac, their frequencies are in general very different. The frequency of transverse betatron oscillation is $(n-\nu_0^{V,H})\omega_0/(2\pi)$, where n is the revolution harmonic closest to the tune. These frequencies are therefore only fractions of the revolution frequency. On the other hand, the axial bunch frequency is a $h\omega_0/(2\pi)$ with h the rf harmonic, which is often many times revolution frequency. For this reason, it is reasonable to consider the ac magnetic fields arising from axial bunching *always non-penetrating*, while the ac magnetic fields arising from betatron oscillation sometimes non-penetrating and sometimes penetrating.

In the expressions below, we try also to include the effect of trapped particles that carry charges of the opposite sign. Take a proton beam, for example, electrons can be trapped, giving a neutralization coefficient χ_e , which is defined as the ratio of the total number of trapped electrons to the total number of protons. (For antiproton beam, the particles trapped are positively charged ions.) The trapped electrons will not travel longitudinally. Therefore, they only affect the electric force but not the magnetic force. In other words, for electric contributions, we replace 1 by $(1 - \chi_e)$.

The incoherent tune shift for a bunched beam is expressed as

$$\Delta\nu_{\text{incoh}}^{V,H} = -\frac{Nr_0R}{\pi\gamma\beta^2\nu_0^{V,H}} \left[\frac{1-\chi_e}{B} \frac{\epsilon_1^{V,H}}{h^2} + \mathcal{F}\beta^2 \frac{\epsilon_2^{V,H}}{g^2} - \beta^2 \left(\frac{1}{B} - 1 \right) \frac{\epsilon_1^{V,H}}{h^2} + (1-\chi_e-\beta^2) \frac{\epsilon_{\text{spch}}^{V,H}}{a_V^2} \right]. \quad (4.43)$$

↑	↑	↑	↑
electric image in vacuum chamber	magnetic image in magnet poles	ac magnetic image from axial bunching	self-field

The second term represents magnetic fields of a stationary beam and its images and

therefore the usual incoherent magnetic image coefficient $\epsilon_2^{V,H}$, which describes dc magnetic fields penetrating the vacuum chamber and landing at the magnet poles. Here, there is no division by the bunching factor B , because we are talking about the dc fields coming from the *average* beam current.

The third term is for the ac magnetic fields generated from axial bunching and a division by B is therefore necessary. Since the ac magnetic fields are non-penetrating, their contribution is the same as that of the incoherent electric field and therefore the factor $-\beta^2\epsilon_1^{V,H}$. We must remember that there is a dc part that lands on the magnet pole faces which we have considered already and must not be included here again. For this reason, we need to replace B^{-1} by $B^{-1} - 1$. The accuracy of this term can be inferred by noticing its disappearance when we let $B \rightarrow 1$, or the bunched beam becomes totally unbunched. After re-arrangement, this incoherent tune shift becomes

$$\Delta\nu_{\text{incoh}}^{V,H} = -\frac{Nr_0R}{\pi\gamma\beta^2\nu_0^{V,H}} \left[\left(\frac{1-\chi_e - \beta^2}{B} + \beta^2 \right) \frac{\epsilon_1^{V,H}}{h^2} + \mathcal{F}\beta^2 \frac{\epsilon_2^{V,H}}{g^2} + (1-\chi_e - \beta^2) \frac{\epsilon_{\text{spch}}^{V,H}}{a_V^2} \right]. \quad (4.44)$$

For coherent motion with penetrating magnetic fields from betatron oscillation, we have

$$\Delta\nu_{\text{coh}}^{V,H} = -\frac{Nr_0R}{\pi\gamma\beta^2\nu_0^{V,H}} \left[\frac{1-\chi_e}{B} \frac{\xi_1^{V,H}}{h^2} + \mathcal{F}\beta^2 \frac{\xi_2^{V,H}}{g^2} - \beta^2 \left(\frac{1}{B} - 1 \right) \frac{\xi_1^{V,H}}{h^2} \right]. \quad (4.45)$$

$$\begin{array}{ccc} \uparrow & \uparrow & \uparrow \\ \text{electric image} & \text{magnetic image} & \text{ac magnetic image} \\ \text{in vacuum chamber} & \text{in magnet poles} & \text{from axial bunching} \end{array}$$

where the third term is contributed by the magnetic field of bunching frequencies, which cannot penetrate the vacuum chamber. The magnetic fields divide into the dc part and the ac part in exactly the same way as Eq. (4.43), the expression for incoherent tune shift. Because we are talking about coherent tune shifts, the coefficients $\epsilon_2^{V,H}$ and $\epsilon_1^{V,H}$ are replaced, respectively by $\xi_2^{V,H}$ and $\xi_1^{V,H}$. After re-arrangement, the coherent tune shifts with penetrating magnetic fields from betatron oscillation becomes

$$\Delta\nu_{\text{coh}}^{V,H} = -\frac{Nr_0R}{\pi\gamma\beta^2\nu_0^{V,H}} \left[\left(\frac{1-\chi_e - \beta^2}{B} + \beta^2 \right) \frac{\xi_1^{V,H}}{h^2} + \mathcal{F}\beta^2 \frac{\xi_2^{V,H}}{g^2} \right]. \quad (4.46)$$

Finally, we come to ac magnetic fields that are non-penetrating coming from both

axial bunching and betatron oscillation. The coherent tune shifts are

$$\Delta\nu_{\text{coh}}^{V,H} = -\frac{Nr_0R}{\pi\gamma\beta^2\nu_0^{V,H}} \left[\frac{1-\chi_e}{B} \frac{\xi_1^{V,H}}{h^2} + \mathcal{F}\beta^2 \frac{\epsilon_2^{V,H}}{g^2} - \beta^2 \frac{\xi_1^{V,H} - \epsilon_1^{V,H}}{h^2} - \beta^2 \left(\frac{1}{B} - 1 \right) \frac{\xi_1^{V,H}}{h^2} \right]. \quad (4.47)$$

↑ ↑ ↑ ↑
 electric image magnetic image ac magnetic image ac magnetic image
 in vacuum chamber in magnet poles from transverse from axial bunching
 motion

Here, the axial bunching parts are very exactly the same as in Eq. (4.45) because they describe exactly the same ac magnetic fields coming from axial bunching. As for the dc magnetic fields, the contribution in Eq. (4.45) comes from both terms of the beam force on the right side of Eq. (4.5) and contributes the coefficient $\xi_2^{V,H}$. Here the dc magnetic fields come from only the first term of the beam force and contribute $\epsilon_1^{V,H}$ instead, for exactly the same reason as in Eq. (4.39). The part of the second term that comes from betatron oscillation of the beam gives rise to the second last term of Eq. (4.47), for exactly the same reason as in Eq. (4.39). After re-arrangement, this coherent tune shift takes the form

$$\Delta\nu_{\text{coh}}^{V,H} = -\frac{Nr_0R}{\pi\gamma\beta^2\nu_0^{V,H}} \left[\frac{1-\chi_e - \beta^2}{B} \frac{\xi_1^{V,H}}{h^2} + \mathcal{F}\beta^2 \frac{\epsilon_2^{V,H}}{g^2} + \beta^2 \frac{\epsilon_1^{V,H}}{h^2} \right]. \quad (4.48)$$

4.3 Other Vacuum Chamber Geometries

The electric and magnetic image coefficients have been computed for other geometries of the vacuum chamber: circular cross section, elliptical cross section [2, 3, 4], and rectangular cross section [5], and even with the beam off-centered. The computations for the rectangular and elliptical cross sections involve one or more than one conformal mappings and the results are given in terms of elliptical functions.

4.3.1 Circular Vacuum Chamber

The situation of circular cross section with an on-center beam is rather simple. Consider a line charge of linear density λ_1 at location $x = 0$ and $y = \bar{y}_1$ inside the cylindric beam pipe of radius b with infinitely conducting walls. We place an image line charge of linear density λ_2 at location $x = 0$ and $y = \bar{y}_2$ as shown in left plot of Fig. 4.5.

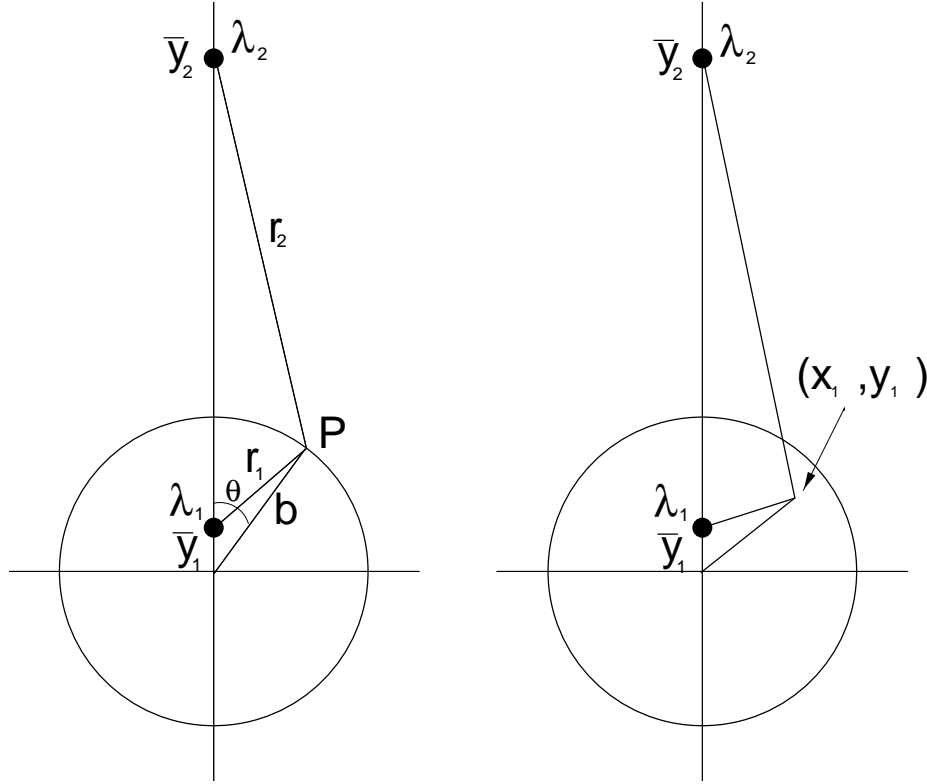


Figure 4.5: Left plot illustrates a line charge density λ_1 inside a cylindrical beam pipe offset vertically by \bar{y}_1 . There is an image line charge density λ_2 at \bar{y}_2 such that the electric potential vanishes at every point P at the beam pipe. Right plot shows the combined electric force acting on a witness line charge at (x_1, y_1) .

The electric potential at point P on a chamber wall at an angle θ is given by

$$V_P = -\frac{e\lambda_1}{2\pi\epsilon_0} \ln r_1 - \frac{e\lambda_2}{2\pi\epsilon_0} \ln r_2 , \quad (4.49)$$

where

$$\begin{cases} r_1^2 = \bar{y}_1^2 + b^2 - 2\bar{y}_1 b \cos \theta , \\ r_2^2 = \bar{y}_2^2 + b^2 - 2\bar{y}_2 b \cos \theta . \end{cases} \quad (4.50)$$

Two assertions are made:

$$\bar{y}_2 = \frac{b^2}{\bar{y}_1} \quad \text{and} \quad \lambda_2 = -\lambda_1 . \quad (4.51)$$

We obtain from the first assertion that $r_2^2 = r_1^2(b^2/\bar{y}_1^2)$. Then the second assertion ensures that the electric potential V_P vanishes aside from a constant for any point on the wall of the cylindrical vacuum chamber.

To compute the image force, place a witness line charge at $x = x_1$ and $y = y_1$, as illustrated in the right plot of Fig. 4.5. The electric force exerted on the witness charge by the image has the y component

$$\frac{F_y^{\text{elec}}}{e} = \frac{e\lambda_1}{2\pi\epsilon_0} \frac{\frac{b^2}{\bar{y}_1} - y_1}{x_1^2 + \left(\frac{b^2}{\bar{y}_1} - y_1\right)^2} \rightarrow \frac{e\lambda_1}{2\pi\epsilon_0} \frac{\bar{y}_1}{b^2}, \quad (4.52)$$

where in the last step only terms linear in y_1 and \bar{y}_1 are retained. According to Eq. (4.13),

$$\Delta\nu_{\text{incoh}}^V = -\frac{Nr_0R}{\pi\gamma\beta^2\nu_0^V} \frac{\epsilon_1^V}{b^2} \quad \text{and} \quad \Delta\nu_{\text{coh}}^V = -\frac{Nr_0R}{\pi\gamma\beta^2\nu_0^V} \frac{\xi_1^V}{b^2}, \quad (4.53)$$

we immediately obtain the incoherent and coherent electric image coefficients for a circular beam pipe:

$$\epsilon_1^V = 0 \quad \text{and} \quad \xi_1^V = \frac{1}{2}. \quad (4.54)$$

Because of the cylindrical symmetry, we also have

$$\epsilon_1^H = 0 \quad \text{and} \quad \xi_1^H = \frac{1}{2}. \quad (4.55)$$

It is not surprising to see the incoherent electric image coefficients vanish. This is because at the point of observation of the witness charge, $\vec{\nabla} \cdot \vec{E} = 0$, leading to $\epsilon_1^V + \epsilon_1^H = 0$.

4.3.2 Elliptical Vacuum Chamber

4.3.2.1 Off-centered Beam

The elliptical cross section of the vacuum chamber has *half width* w and *half height* $h < w$. They are also known as the major and minor radii. The focal points are on the horizontal axis at distance $\varepsilon = \sqrt{w^2 - h^2}$ from the center. Consider a line beam on the horizontal axis at distance x from the center. The image coefficients can be obtained by performing two conformal mappings [2, 3, 4]. The derivations are rather involved. Here, we only present the results. When the beam is inside the focal points[†] or $0 < x < \varepsilon$,

$$\epsilon_1^V = -\epsilon_1^H = \frac{h^2}{12W^2} \left[A \left(\frac{2K}{\pi \operatorname{cn} \operatorname{dn}} \right)^2 + \frac{6Kk'^2 x \operatorname{sn}}{\pi W \operatorname{cn} \operatorname{dn}} - \frac{4\varepsilon^2 + 5x^2}{2W^2} \right], \quad (4.56)$$

[†]These expressions are presented from Eqs. (74) to (76) in Ref. [3]. The expression following Eq. (74) is incorrect that the factor $(1 + k^2 + k^4)$ in the middle term should have been $(1 + 2k^2 + k^4)$. The first factor in Eq. (76) after the opening square bracket, $(1 - k^2 S^2)$, should have been $(1 - k^2 S^4)$.

$$\xi_1^V = \frac{h^2}{4W^2} \left[\left(\frac{2K \operatorname{dn}}{\pi \operatorname{cn}} \right)^2 + \frac{2Kk'^2 x \operatorname{sn}}{\pi W \operatorname{cn} \operatorname{dn}} - \frac{\varepsilon^2 + x^2}{W^2} \right], \quad (4.57)$$

$$\xi_1^H = -\frac{h^2}{4W^2} \left[(1 - k^2 \operatorname{sn}^4) \left(\frac{2Kk'}{\pi \operatorname{cn} \operatorname{dn}} \right)^2 + \frac{2Kk'^2 x \operatorname{sn}}{\pi W \operatorname{cn} \operatorname{dn}} - \frac{\varepsilon^2 + x^2}{W^2} \right], \quad (4.58)$$

where

$$A = (2 - k^2) - \frac{1}{2}(1 + k^2)^2 \operatorname{sn}^2 - k^2(1 - 2k^2) \operatorname{sn}^4, \quad (4.59)$$

and

$$W^2 = \varepsilon^2 - x^2 = w^2 - h^2 - x^2. \quad (4.60)$$

The arguments of the Jacobian elliptic functions sn , cn , dn are

$$\left(\frac{2K(k)}{\pi} \sin^{-1}(x/\varepsilon), k \right), \quad (4.61)$$

where $K = K(k)$ is the complete elliptical function of the first kind and k is called the *modulus*[‡]. The complementary modulus k' is given by

$$k' = \sqrt{1 - k^2}. \quad (4.62)$$

We first compute the *nome*, defined as

$$q = \exp \left[-\frac{\pi K'(k)}{K(k)} \right], \quad (4.63)$$

using the expression

$$q = \frac{w - h}{w + h}, \quad (4.64)$$

then the complementary modulus k' using[§]

$$k'^{\frac{1}{2}} = \frac{1 + 2 \sum_{s=1}^{\infty} (-1)^s q^{s^2}}{1 + 2 \sum_{s=1}^{\infty} q^{s^2}}, \quad (4.65)$$

and finally the modulus k through Eq. (4.62).

[‡]Some authors also define the *parameter* $m = k^2$ and the *complementary parameter* $m' = k'^2 = 1 - m$.

[§]This formula was stated wrongly in Eq. (6) of Ref. [5].

Notice that each term in Eqs. (4.56), (4.57), and (4.58) becomes singular when the beam approaches the focal points of the elliptic cross section. However, the singularities cancel each other in each expression to arrive at a finite value as $x \rightarrow \varepsilon$. For this reason double precision must be used in evaluating these expressions. Right at the focal points the image coefficients become[¶]

$$\epsilon_1^V = -\epsilon_1^H = \frac{h^2}{360\varepsilon^2} \left[(1 - 16k^2 + k^4) \left(\frac{2K}{\pi} \right)^4 + 10(1 + k^2) \left(\frac{2K}{\pi} \right)^2 - 11 \right], \quad (4.66)$$

$$\xi_1^V = \frac{h^2}{180\varepsilon^2} \left[(2 + 13k^2 + 2k^4) \left(\frac{2K}{\pi} \right)^4 + 5(1 + k^2) \left(\frac{2K}{\pi} \right)^2 - 7 \right], \quad (4.67)$$

$$\xi_1^H = \frac{-h^2}{180\varepsilon^2} \left[2(1 - 16k^2 + k^4) \left(\frac{2K}{\pi} \right)^4 + 5(1 + k^2) \left(\frac{2K}{\pi} \right)^2 - 7 \right]. \quad (4.68)$$

When the beam is outside the focal points or $x > \varepsilon$, the image coefficients assume the form^{||}

$$\epsilon_1^V = -\epsilon_1^H = \frac{h^2}{12W^2} \left[B_1 \left(\frac{2K}{\pi \operatorname{sn} \operatorname{cn}} \right)^2 + \frac{6Kx \operatorname{dn}}{\pi W \operatorname{sn} \operatorname{cn}} - \frac{4\varepsilon^2 + 5x^2}{2W^2} \right], \quad (4.69)$$

$$\xi_1^V = \frac{h^2}{4W^2} \left[\left(\frac{2K \operatorname{cn}}{\pi \operatorname{sn}} \right)^2 + \frac{2Kx \operatorname{dn}}{\pi W \operatorname{sn} \operatorname{cn}} - \frac{\varepsilon^2 + x^2}{W^2} \right], \quad (4.70)$$

$$\xi_1^H = -\frac{h^2}{4W^2} \left[B_2 \left(\frac{2K}{\pi \operatorname{sn} \operatorname{cn}} \right)^2 + \frac{2Kx \operatorname{dn}}{\pi W \operatorname{sn} \operatorname{cn}} - \frac{\varepsilon^2 + x^2}{W^2} \right], \quad (4.71)$$

where

$$B_1 = \frac{3}{2} - \frac{1}{2}(8 - k'^2) \operatorname{sn}^2 + (1 + k'^2) \operatorname{sn}^4, \quad B_2 = 1 - 2 \operatorname{sn}^2 + k'^2 \operatorname{sn}^4. \quad (4.72)$$

Unlike the situation when the beam is inside the focal points, here

$$W^2 = x^2 - \varepsilon^2 = x^2 - w^2 + h^2, \quad (4.73)$$

[¶]in Ref. [3], in Appendix D(f), the first term of ξ_1^V was $(2 - 13k^2 + 2k^4)$ which has a wrong sign preceding $13k^2$ as compared with our Eq. (4.67). In Ref. [4], Table II, Part (c), the expression for ϵ_1 when $x = \varepsilon$, has an overall incorrect sign.

^{||}In Ref. [3], Appendix D(e), the expressions for ϵ_1^V , ξ_1^V , and ξ_1^H all have negative signs in front of the middle terms inside the square brackets. They should be all positive as given by Eqs. (4.69), (4.70), and (4.71). The expression for B_1 in Ref. [3] has the typo that S in the second term on the right side should have been S^2 .

and the Jacobian elliptic functions sn , cn , and dn have arguments

$$\left(\frac{2K(k)}{\pi} \cosh^{-1}(x/\varepsilon), k' \right) . \quad (4.74)$$

However, the nome q , modulus k , and complementary modulus k' are the same as given by Eqs. (4.64), (4.62), and (4.65).

4.3.2.2 Centered Beam

When the beam is right at the center of the vacuum chamber, $x = 0$. The arguments of the elliptic functions in Eq. (4.61) simplify to $(0, k)$ and we have $\text{sn} = 0$, $\text{cn} = \text{dn} = 1$. The expressions for the image coefficients in Eqs. (4.56), (4.57), and (4.58) simplify readily to

$$\epsilon_1^V = -\epsilon_1^H = \frac{h^2}{12\varepsilon^2} \left[(1 + k'^2) \left(\frac{2K}{\pi} \right)^2 - 2 \right] , \quad (4.75)$$

$$\xi_1^V = \frac{h^2}{4\varepsilon^2} \left[\left(\frac{2K}{\pi} \right)^2 - 1 \right] , \quad (4.76)$$

$$\xi_1^H = \frac{h^2}{4\varepsilon^2} \left[1 - \left(\frac{2Kk'}{\pi} \right)^2 \right] . \quad (4.77)$$

4.3.3 Rectangular Vacuum Chamber

4.3.3.1 Off-Centered Beam

To conform with the elliptical beam pipe, let h and w be, respectively, the *half height* and *half width* of the rectangular cross section**. When the beam is on the horizontal axis but with fractional offset g (or at distance gw from the center), the image coefficients are††

$$\epsilon_1^V = -\epsilon_1^H = \frac{K^2(k)}{4} \left[\frac{k'^4 \text{sn}^2 \text{cn}^2}{2 \text{dn}^2} - \frac{k'^2(1 - 2 \text{sn}^2)}{3} - \frac{\text{dn}^2(3 - 4 \text{sn}^2 + 4 \text{sn}^4)}{6 \text{sn}^2 \text{cn}^2} \right] , \quad (4.78)$$

**Note that in Ref. [5], h and w are the *full height* and *full width* of the rectangular cross section.

††Equation (4.78) was reported in Eq. (53) of Ref. [5] with a wrong sign in front of sn_{10}^4 inside the last term in the curly brackets.

$$\xi_1^V = \frac{K^2(k)}{4} \frac{k'^4 \operatorname{sn}^2 \operatorname{cn}^2}{\operatorname{dn}^2}, \quad (4.79)$$

$$\xi_1^H = \frac{K^2(k)}{4} \left[k'^2 (1 - 2 \operatorname{sn}^2) + \frac{\operatorname{dn}^2}{\operatorname{sn}^2 \operatorname{cn}^2} \right]. \quad (4.80)$$

The arguments of the elliptic functions sn , cn , dn are

$$\left(\frac{K(k)y_0}{h}, k' \right) = \left(\frac{K(k)w}{h}(1-g), k' \right), \quad (4.81)$$

where $y_0 = (1-g)w$ is the position of the beam measured from one vertical wall of the vacuum chamber, and $K(k)$ is the complete elliptical function of the first kind.

Here, the nome is computed according to

$$q = e^{-2\pi w/h}, \quad (4.82)$$

which is quite different from the one used in Eq. (4.64) for the elliptical beam pipe. Next, the complementary modulus k' can be computed from Eq. (4.65), from which the modulus k can be obtained via Eq. (4.62).

4.3.3.2 Centered Beam

For a centered beam, $g = 0$, the arguments of the elliptical functions become

$$\left(\frac{K(k)w}{h}, k' \right) = \left(\frac{1}{2} K'(k), k' \right) = \left(\frac{1}{2} K(k'), k' \right). \quad (4.83)$$

Notice that the periods of sn , cn , dn with modulus k' are $4K(k')$. The elliptical functions simplify to [6]

$$\operatorname{sn}\left(\frac{1}{2}K(k'), k'\right) = \frac{1}{\sqrt{1+k}}, \quad \operatorname{cn}\left(\frac{1}{2}K(k'), k'\right) = \frac{\sqrt{k}}{\sqrt{1+k}}, \quad \operatorname{dn}\left(\frac{1}{2}K(k'), k'\right) = \sqrt{k}. \quad (4.84)$$

The electric image coefficients simplify to

$$\epsilon_1^V = -\epsilon_1^H = \frac{K^2(k)}{12} (1 - 6k + k^2), \quad (4.85)$$

$$\xi_1^V = \frac{K^2(k)}{4} (1 - k)^2, \quad (4.86)$$

$$\xi_1^H = K^2(k) k, \quad (4.87)$$

which involve only the complete elliptical function of the first kind.

4.3.3.3 Comments

1. Since q decreases exponentially as w/h increases, very accurate value of k' can be computed with Eq. (4.65). For example, even for $1 \geq w/h \geq 0.2$, 14-figure accuracy can be readily obtained for k' and also k^2 afterward using Eq. (4.62), when the summations are extended to $s = 5$. In fact, for centered beam, there is no need to go to $w/h < 1$, because we can interchange the role of w and h .
2. When $w/k > 1$, q becomes very small and k' is very close to 1. (For example, $k^2 = 2.9437 \times 10^{-3}$, 5.5796×10^{-5} and 1.0420×10^{-7} , respectively, when $w/h = 1$, 2 and 3.) Equation (4.62) can no longer give accurate result for k . To preserve accuracy, we must expand k^2 as power series in q with the aid of Eqs. (4.62) and (4.65):

$$k^2 = 16q(1 - 8q + 44q^2 - 192q^3 + 718q^4 - 2400q^5 + 7352q^6 - 20992q^7 + 56549q^8 - \dots) , \quad (4.88)$$

from which 14-figure accuracy can be obtained when $w/k \geq 1$.

3. Because $k^2 \ll 1$ when $w/h > 1$, Eqs. (4.85), (4.86), and (4.87) can be viewed as expansions from values for the infinite horizontal plates. In fact, with

$$K(k) = \frac{\pi}{2} \left[1 + \frac{1}{4}k^2 + \frac{9}{64}k^4 + \mathcal{O}(k^6) \right] , \quad (4.89)$$

we can write

$$\epsilon_1^V = -\epsilon_1^H = \frac{\pi^2}{48} \left[1 - 6k + \frac{3}{2}k^2 - 3k^3 + \frac{27}{32}k^4 - \frac{33}{16}k^5 + \mathcal{O}(k^6) \right] , \quad (4.90)$$

$$\xi_1^V = \frac{\pi^2}{16} \left[1 - 2k + \frac{3}{2}k^2 - k^3 + \frac{27}{32}k^4 - \frac{11}{16}k^5 + \mathcal{O}(k^6) \right] , \quad (4.91)$$

$$\xi_1^H = \frac{\pi^2}{4} k \left[1 + \frac{1}{2}k^2 + \frac{11}{32}k^4 + \mathcal{O}(k^6) \right] . \quad (4.92)$$

4.3.4 Closed Yoke

Mathematically, it is impossible to compute the magnetic image coefficients for a closed cylindrical iron yoke that has infinite relative permeability. In fact, no solution exists

for a closed iron yoke of any geometry. This is because Ampere's law requires

$$\oint \vec{H} \cdot d\vec{\ell} = I . \quad (4.93)$$

For a beam of current I , the component of magnetic field \vec{H} along the inner surface of the iron yoke is therefore nonzero. Thus, the magnetic flux density \vec{B} inside the yoke becomes infinite. Speaking in the reverse order, if the magnetic flux density inside the yoke is finite, the magnetic field \vec{H} along the inner surface must vanish. From Ampere's law, one gets $I = 0$, or no current is allowed to flow through the yoke.

For a normal-temperature magnet, we like to operate in the linear region of the B - H hysteresis curve, for example at Point N in Fig. 4.6, in order to take advantage of

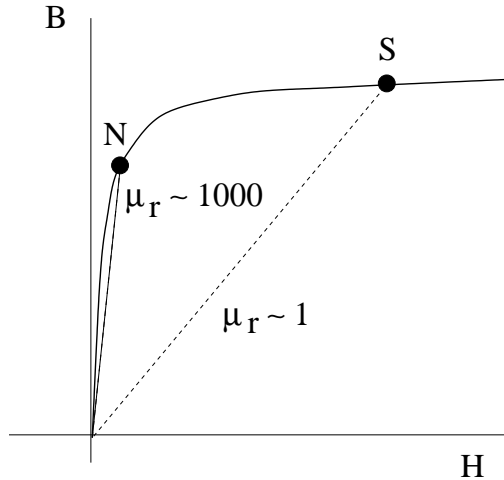


Figure 4.6: B - H hysteresis plot showing the operation of normal temperature magnet at Point N where the relative magnetic permeability μ_r is large. The operation of superconducting magnet is at Point S where the iron yoke is at saturation and $\mu_r \approx 1$.

the large relative magnetic permeability, $\mu_r \sim 1000$. Then, most of the magnetic flux density across the pole gap is supplied by μ_r and only a few percents come from the winding current. Such operation limits the magnetic flux density to $B_{\max} \sim 1.8$ T. This explains why the iron yoke is mostly made up of two pieces glued together with some medium. In that case, \vec{H} will only be large in the medium but relatively small inside the yoke and a much larger beam current will be allowed.

The story for superconducting magnets is quite different. Here, the magnetic flux density is mostly supplied by the high winding current, while the iron yoke is always

saturated. The operation point in the hysteresis curve is now at S of Fig. 4.6 in the large H region where the local slope is 1. Thus the relative permeability μ_r becomes close to 1 and is very much less than the linear region of the hysteresis curve. If a closed iron yoke is used, the maximum beam current allowed by Ampere's law becomes $\mu_r \sim 1000$ times larger at operation point S than at operation point N .

When the relative permeability is finite, the Laplace equation can still be solved using the image method, provided there is sufficient symmetry in the geometry. Readers with interest are referred to, for example, the book by Binns and Lawrenson [7].

In Table 4.2, we tabulate the self-field coefficients for uniformly charged beams and image coefficients for centroid beams [8].

4.4 Connection with Impedance

In Eq. (4.5), the term proportional to y on the right side is absorbed into the betatron tune shift so that ν_0^V becomes ν_V . The equation becomes

$$\frac{d^2y}{ds^2} + \frac{(\nu^V)^2}{R^2}y = \frac{1}{\gamma mv^2} \left. \frac{\partial \langle F_{\text{beam}}(y, \bar{y}) \rangle}{\partial \bar{y}} \right|_{y=0} \bar{y}. \quad (4.94)$$

The coherent force on the right is related to the transverse wake function and therefore the transverse impedance. The connection can be easily made using Eq. (1.28), which says

$$\left. \frac{\partial \langle F_{\text{beam}}(y, \bar{y}) \rangle}{\partial \bar{y}} \right|_{y=0} \bar{y} = \frac{ieZ_1^\perp \beta I \bar{y}}{C} = \frac{ie^2 Z_1^\perp \beta^2 c \lambda \bar{y}}{C}. \quad (4.95)$$

On the other hand, in Eq. (4.12), according to the definition of the image coefficient,

$$eE^V(y, \bar{y})|_{y=0} = \frac{e^2 \lambda Z_0 c}{\pi} \frac{\xi_1^V - \epsilon_1^V}{h^2} \bar{y}. \quad (4.96)$$

As a result, we obtain

$$Z_1^\perp = -i \frac{Z_0 C}{\pi \gamma^2 \beta^2} \frac{\xi_1^V - \epsilon_1^V}{h^2}. \quad (4.97)$$

For a circular beam pipe, $\xi_1^V = \frac{1}{2}$ and $\epsilon_1^V = 0$. This is just exactly the second half of the transverse space charge impedance in Eq. (1.38). Thus, the transverse space charge impedance can be interpreted as the summation of two parts: the part proportional

Table 4.2: Self-field coefficients for uniformly charged beam and image coefficients for centered beam.

Coeff.	Circular	Elliptical	Rectangular	Parallel Plates
ϵ_{spch}^V	$\frac{1}{2}$	$\frac{a_V}{a_H + a_V}$		
ϵ_{spch}^H	$\frac{1}{2}$	$\frac{a_V^2}{a_H(a_H + a_V)}$		
ϵ_1^V	0	$\frac{h^2}{12\varepsilon^2} \left[(1+k'^2) \left(\frac{2K}{\pi} \right)^2 - 2 \right]$	$\frac{K^2(k)}{12} (1 - 6k + k^2)$	$\frac{\pi^2}{48}$
ϵ_1^H	0	$\frac{-h^2}{12\varepsilon^2} \left[(1+k'^2) \left(\frac{2K}{\pi} \right)^2 - 2 \right]$	$\frac{-K^2(k)}{12} (1 - 6k + k^2)$	$-\frac{\pi^2}{48}$
ϵ_2^V	*	*	*	$\frac{\pi^2}{24}$
ϵ_2^H	*	*	*	$-\frac{\pi^2}{24}$
ξ_1^V	$\frac{1}{2}$	$\frac{h^2}{4\varepsilon^2} \left[\left(\frac{2K}{\pi} \right)^2 - 1 \right]$	$\frac{K^2(k)}{4} (1 - k)^2$	$\frac{\pi^2}{16}$
ξ_1^H	$\frac{1}{2}$	$\frac{h^2}{4\varepsilon^2} \left[1 - \left(\frac{2Kk'}{\pi} \right)^2 \right]$	$K^2(k)k$	0
ξ_2^V	*	*	*	$\frac{\pi^2}{16}$
ξ_2^H	*	*	*	0

* ϵ_2 and ξ_2 for closed magnetic boundary (e.g., circular, elliptic, or rectangular) cannot be calculated when the relative permeability $\mu_r \rightarrow \infty$, since the induced magnetic field would not permit a charged beam to pass through because the field energy would become infinite. Closed magnetic yokes are used in superconducting magnets, but there the coefficients $\epsilon_2 = \xi_2 \rightarrow 0$, since the magnetic material is driven completely into saturation ($\mu_r \rightarrow 1$).

$K(k)$ is the complete elliptic integral of the first kind. k is determined from $(w-h)/(w+h) = \exp(-\pi K'/K)$ for the elliptical cross section but $w/h = K'/(2K)$ for the rectangular cross section, where w and h are the half width and half height, with $\varepsilon = \sqrt{w^2 - h^2}$, and $K' = K(k')$ with $k' = \sqrt{1 - k^2}$.

to a^{-2} is the self-field contribution and the part proportional to b^{-2} is the wall image contribution. We can therefore rewrite the expression in a more general form

$$Z_1^{V,H} = i \frac{Z_0 C}{\pi \gamma^2 \beta^2} \left[\frac{\epsilon_{\text{spch}}^{V,H}}{a_v^2} - \frac{\xi_1^{V,H} - \epsilon_1^{V,H}}{h^2} \right], \quad (4.98)$$

where h is the half height of the vacuum chamber.

It is important to distinguish the difference between the force generating the coherent tune shift and the force generating the transverse impedance. The former involves the ξ_1 coefficient while the later involves $\xi_1 - \epsilon_1$. The coherent tune shift is the result of all forces acting on the center of the beam \bar{y} , while the transverse impedance comes from the force generated by the center motion of the beam on an individual particle. In other words,

$$\begin{aligned} \Delta\nu &\propto \frac{\partial \langle F_{\text{beam}}(y, \bar{y}) \rangle}{\partial y} \Big|_{\bar{y}=0} + \frac{\partial \langle F_{\text{beam}}(y, \bar{y}) \rangle}{\partial \bar{y}} \Big|_{y=0}, \\ Z_1^\perp &\propto \frac{\partial \langle F_{\text{beam}}(y, \bar{y}) \rangle}{\partial \bar{y}} \Big|_{y=0}. \end{aligned} \quad (4.99)$$

Thus, the results can be very different. Take the example of a beam between two infinite conducting planes. Because of horizontal translational invariance, the horizontal force acting at the center of the beam vanishes independent of whether the beam is moving horizontally or vertically. The horizontal coherent tune shift therefore vanishes. However, the horizontal motion of the center of mass of the beam does provide a horizontal force on an individual particle, which may not be moving with the center of mass. That individual particle will therefore see a nonvanishing transverse impedance.

4.5 More about Wake Functions

Most of the time the vacuum chamber is not cylindrical in shape. Thus, the expansion into circular harmonics in Sec. 1.4 cannot be performed. Here, we want to emphasize that it is always completely valid to expand \vec{E} and \vec{B} into circular harmonics. However, when the boundary conditions are applied, \vec{E} and \vec{B} of different circular harmonics will be mixed together, and so are the wake functions W_m for different m 's. In other words, equations corresponding to an individual m are not independent, thus rendering the expansion useless. For this reason, we need to give slightly different definitions for the wake functions when there is no cylindrical symmetry.

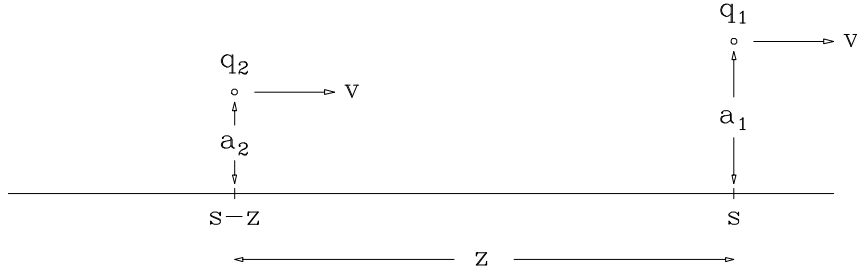


Figure 4.7: Test particle with charge q_1 at an offset of a_1 from the designated path leaves wake fields to the witness particle with charge q_2 at an offset of a_2 at a distance z behind.

Consider a test particle carrying charge q_1 traveling with velocity v longitudinally along a designated path in a vacuum chamber. A witness particle of charge q_2 at a distance z behind along the same path sees a longitudinal force F_0^{\parallel} and a transverse force F_0^{\perp} due to the wake fields of the test particle. In general, these forces depend also on the location s of the test particle along the beam pipe. However, when we apply the impulse approximation, these forces are integrated over s for a long length ℓ of the beam pipe and become functions of z only. For a circular machine, ℓ is taken as the circumference C . Unlike the situation of traveling along the symmetry axis of a cylindrical beam pipe, here there is always an average transverse force $\langle F_0^{\perp} \rangle$. This transverse force comes mostly from the images in the walls of the vacuum chamber. It should be weak in general and can therefore be incorporated into the betatron tunes as tune shifts in the way discussed above in Sec. 4.1.

The *longitudinal wake function* is defined as

$$W'_0(z) = -\frac{\langle F_0^{\parallel} \rangle \ell}{q_1 q_2}, \quad (4.100)$$

where $\langle F_0^{\parallel} \rangle \ell$ denotes the longitudinal integrated wake force or impulse.

If the path of the source particle is displaced transversely by a_1 from the designated path as in Fig. 4.7, the witness particle displaced by a_2 at a distance z behind will see a longitudinal force F_1^{\parallel} and a transverse force F_1^{\perp} . The *transverse wake function* is now defined by

$$W_1(z) = -\lim_{a_1, a_2 \rightarrow 0} \frac{(\langle F_1^{\perp} \rangle - \langle F_0^{\perp} \rangle) \ell}{a_1 q_1 q_2}, \quad (4.101)$$

where the transverse force along the designated path $\langle F_0^{\perp} \rangle$ has been subtracted away

because it has been taken care of already as tune shifts. Defined in this way, $W'_0(z)$ and $W_1(z)$ will be the same as the $m = 0$ longitudinal wake function and the $m = 1$ transverse wake function defined in Chapter 1.

4.6 Exercises

4.1. Consider a beam with bi-parabolic or semi-circular distribution

$$\rho(r) = \frac{2e\lambda}{\pi\hat{r}^2} \left(1 - \frac{r^2}{\hat{r}^2}\right), \quad (4.102)$$

where \hat{r} is the radial extent of the beam and λ is the linear particle density.

- (1) Compute the self-field or space charge incoherent tune shift at the center of the beam where it is maximal and show that the space charge coefficient defined in Eq. (4.25) is $\epsilon_{\text{spch}} = 1$.
- (2) Explain how one can understand that ϵ_{spch} for this distribution is in between $\epsilon_{\text{spch}} = \frac{1}{2}$ for uniform distribution and $\epsilon_{\text{spch}} \approx \frac{3}{2}$ for bi-Gaussian distribution.

4.2. The horizontal betatron tune shift due to a quadrupole gradient error $\Delta k(s) = \Delta B'_V/(B\rho)$ at location s along the accelerator ring is

$$\Delta\nu_{\beta_H} = \frac{1}{4\pi} \int_0^C \beta_H(s) \Delta k(s) ds, \quad (4.103)$$

where β_H is the betatron function, C is the circumference of the ring, $\Delta B'_V$ is the vertical quadrupole gradient error, and $(B\rho)$ is the magnetic rigidity. Consider the space charge self-force as a quadrupole gradient error, derive, using the above formula, the incoherent dipole space charge tune shift, Eq. (4.24), inside a beam of uniform transverse distribution.

4.3. Consider a beam with elliptic cross section and uniform particle distribution.

- (1) Show that the electric potential

$$V(x, y) = -\frac{e\lambda}{2\pi\epsilon_0} \frac{1}{a_H + a_V} \left(\frac{x^2}{a_H} + \frac{y^2}{a_V}\right) \quad (4.104)$$

for $x^2/a_H^2 + y^2/a_V^2 < 1$ and 0 otherwise, satisfies the Laplace equation

$$\nabla^2 V(x, y) = -\frac{e\lambda}{\pi\epsilon_0 a_H a_V}, \quad (4.105)$$

where λ is the linear particle density of the beam.

- (2) Show that inside the beam, the transverse electric fields are

$$E_x = \frac{e\lambda}{\pi\epsilon_0} \frac{x}{a_H(a_H + a_V)}$$

$$E_x = \frac{e\lambda}{\pi\epsilon_0} \frac{y}{a_V(a_H + a_V)} \quad (4.106)$$

(3) Comparing with the electric field components inside a cylindrically symmetric beam of radius a , show that the space charge tune shift coefficients, defined in Eq. (4.25), inside this beam of elliptic cross section are

$$\epsilon_{\text{spch}}^H = \frac{a_V^2}{a_H(a_H + a_V)} \quad \text{and} \quad \epsilon_{\text{spch}}^V = \frac{a_V}{a_H + a_V} . \quad (4.107)$$

4.4. We are going to derive the electric potential $V(x, y, z)$ for a 3-dimensional charge distribution,

$$\rho(x, y, z) = \frac{eN}{(2\pi)^{3/2}\sigma_x\sigma_y\sigma_z} \exp\left[-\frac{x^2}{2\sigma_x^2} - \frac{y^2}{2\sigma_y^2} - \frac{z^2}{2\sigma_z^2}\right] , \quad (4.108)$$

following the method of Takayama [9], where N is the total number of particles.

(1) Show that the Green function of the Laplace equation can be written as

$$G(\vec{r}, \vec{\xi}) = \frac{1}{4\pi|\vec{r} - \vec{\xi}|} = \frac{1}{2\pi^{3/2}} \int_0^\infty dq e^{-|\vec{r} - \vec{\xi}|^2 q^2} . \quad (4.109)$$

In other words, $G(\vec{r}, \vec{\xi})$ satisfies

$$\nabla^2 G(\vec{r}, \vec{\xi}) = -\delta(\vec{r} - \vec{\xi}) . \quad (4.110)$$

(2) Changing the variable of integration to $t = q^{-2}$, show that the electric potential can be written as

$$V(x, y, z) = \frac{1}{4\pi^{3/2}\epsilon_0} \int_0^\infty \frac{dt}{t^{3/2}} \int_{-\infty}^\infty d\vec{\xi} \rho(\vec{\xi}) e^{-|\vec{r} - \vec{\xi}|^2/t} . \quad (4.111)$$

(3) With ρ given by Eq. (4.108), derive the electric potential

$$V(x, y, z) = \frac{eN}{4\pi^{3/2}\epsilon_0} \int_0^\infty dt \frac{\exp\left[-\frac{x^2}{(2\sigma_x^2+t)} - \frac{y^2}{(2\sigma_y^2+t)} - \frac{z^2}{(2\sigma_z^2+t)}\right]}{\sqrt{(2\sigma_x^2+t)(2\sigma_y^2+t)(2\sigma_z^2+t)}} . \quad (4.112)$$

4.5. Consider a beam with bi-Gaussian transverse charge distribution,

$$\rho(x, y) = \frac{e\lambda}{2\pi\sigma_x\sigma_y} \exp\left(-\frac{x^2}{2\sigma_x^2} - \frac{y^2}{2\sigma_y^2}\right) , \quad (4.113)$$

where σ_x and σ_y are the rms width and height, and λ is the linear particle density.

(1) From Eq. (4.112), show that the electric potential is

$$V(x, y) = \frac{e\lambda}{4\pi\epsilon_0} \int_0^\infty dt \frac{\exp\left[-\frac{x^2}{(2\sigma_x^2+t)} - \frac{y^2}{(2\sigma_y^2+t)}\right]}{\sqrt{(2\sigma_x^2+t)(2\sigma_y^2+t)}}. \quad (4.114)$$

(2) Show that the transverse electric fields are

$$E_x = \frac{e\lambda x}{4\pi\epsilon_0} \int_0^\infty dt \frac{\exp\left[-\frac{x^2}{(2\sigma_x^2+t)} - \frac{y^2}{(2\sigma_y^2+t)}\right]}{(2\sigma_x^2+t)\sqrt{(2\sigma_x^2+t)(2\sigma_y^2+t)}},$$

$$E_y \rightarrow E_x \quad \text{with } x \rightarrow y, \quad y \rightarrow x. \quad (4.115)$$

(3) The self-field or space charge tune shifts are at their maxima at the center of the beam, or $x \rightarrow 0$ and $y \rightarrow 0$. Show that they are given by Eq (4.33) with

$$\sigma^2 \rightarrow \frac{\sigma_x(\sigma_x + \sigma_y)}{2} \quad \text{for } \Delta\nu_{\text{spch incoh}}^H$$

$$\sigma^2 \rightarrow \frac{\sigma_y(\sigma_x + \sigma_y)}{2} \quad \text{for } \Delta\nu_{\text{spch incoh}}^V. \quad (4.116)$$

4.6. Derive the lowest order space charge self-force coefficient ϵ_{spch} of a particle with betatron amplitude r inside a cylindrical symmetric coasting beam with transverse bi-Gaussian distribution.

Answer: $\epsilon_{\text{spch}} = \frac{1}{2}f(r/\sigma_r)$ where σ_r is the rms beam radius and the form factor $f(r/\sigma_r)$ is given by Eq. (4.38).

Bibliography

- [1] L.J. Laslett, Proceedings of 1963 summer Study on Storage Rings, BNL-Report 7534, p. 324; L.J. Laslett and L. Resegotti, Proceedings of VIth Int. Conf. on High Energy Accelerators, Cambridge, MA, 1967, p. 150.
- [2] B. Zotter, CERN Reports ISR-TH/72-8 (1972); IST-TH/74-38 (1974); ISR-TH/75-17 (1975); Proceedings of VIth National particle Accelerator Conf., Washington DC, 1974 (IEEE, 1975).
- [3] B. Zotter, Nucl. Instru. Meth. **129**, 377 (1975).
- [4] B. Zotter, CERN Report ISR-TH/74-11 (1974).
- [5] K.Y. Ng, Particle Accelerators **16**, 63 (1984).
- [6] See, for example, Table 16.5, p.571 of Abramowitz and Stegun, Handbook of Mathematical Functions, Dover, 1965.
- [7] K.J. Binns and P.J. Lawrenson, *Analysis and Computation of Electric and Magnetic Field Problems*, 2nd Ed., Pergamon Press, 1973.
- [8] G. Guignard, CERN 77-10 (1977).
- [9] K. Takayama, Lett. Al Nuovo Cimento **34**, 190 (1982).

